Anisotropy of the Optical Constants and the Band Structure of Graphite

D. L. GREENAWAY AND G. HARBEKE
Laboratories RCA Ltd., Zurich, Switzerland

AND

F. BASSANI AND E. TOSATTI
Università di Pisa and Scuola Normale Superiore, Pisa, Italy

(Received 25 October 1968)

Detailed experimental results have been obtained on the reflectivity of both natural and pyrolytic graphite single crystals in the visible and ultraviolet regions. Results have been taken for both $E\perp c$ and $E\|c$ at near-normal incidence, and as a function of angle of incidence for radiation having its electric vector both perpendicular and parallel to the plane of incidence. These latter results, used in conjunction with an analysis of the Fresnel relations for anisotropic materials, permit extremely accurate values of the optical constants to be obtained both parallel and perpendicular to the crystal planes. The results show that k_z, the absorption index perpendicular to the cleavage planes, is identically equal to zero at all energies below about 5 eV, as expected from the two-dimensional approximation of the energy bands in graphite. A three-dimensional calculation is performed to explain the above picture. The optical constants here obtained explain the electron-energy-loss experiments on graphite and require the absence of the low-energy plasmon along the c axis. The newly developed Fresnel analysis presented here can find general application to all highly anisotropic materials.

I. INTRODUCTION

THE use of the Fresnel relations, coupled with reflectivity measurements as a function of angle of incidence, for the determination of optical constants is clearly not a new technique, but such measurements have been largely restricted to isotropic materials (see, for example, the early work of Avery[1,2]), and in addition such measurements are liable to large inaccuracies for values of the absorption index much less than unity. The now classical method of optical-constant determination for band-structure investigation—normal incidence reflectivity measurements over a wide energy range and a subsequent Kramers-Kronig analysis of the results—is of little value for highly anisotropic materials such as graphite because of the difficulty of preparing reliable measurement surfaces perpendicular to the easy-cleavage planes. With these considerations in mind we have analyzed the Fresnel relations for an anisotropic material and developed a best-fit method of numerical analysis to yield the optical constants from reflectivity data as a function of angle of incidence for cleavage-plane measurements. The difficulty of obtaining absolute values of the reflectivity, particularly at large angles of incidence, when using a conventional spectrometer has been overcome by using gas lasers to provide extremely precise Fresnel curves at a few selected wavelengths (e.g., 6328, 5145, and 4579 Å), and then applying any necessary correction factor to the spectrometer results.

An exact determination of the optical constants for anisotropic materials from the Fresnel relations first formulated by Drude[3] is in principle possible, but the calculation is formidable. The complexity of the calculation has resulted in little use being made of the method for noncubic materials. In 1964, however, Jacobsen formulated a reiterative scheme for the solution of the Fresnel relations for a biaxial crystal[4]; the method was applied successfully to V_2O_5,[5] but it is a somewhat difficult experiment to perform as it depends on ellipsometric measurements to establish the various reflection coefficients. The method we report here for uniaxial materials has been simplified, and in particular can be applied to reflectivity measurements regardless of the phase relationship between the reflected amplitudes parallel and perpendicular to the plane of incidence.

For the present work we have considered the case of graphite, but it should be stressed that our method is a general one and can be applied to any of the highly anisotropic layer compounds whose optical properties have lately been receiving attention, e.g., PbI_2, CdI_2, MoS_2, and ZrS_2.

The anisotropy of the optical constants of graphite has already been investigated by a number of workers. McCartney and Ergun, for example,[6] measured the reflectance of natural crystals at normal incidence in differing immersion media from the $10\bar{1}2$ face and reported maximum and minimum values of refractive and absorptive indices at 5461 Å. In later work, Ergun[7] obtained the more precise values of $n_x=2.15$, $n_z=1.81$ and $k_x=1.42$, $k_z\simeq 0$, also at 5461 Å; these results indicate the marked anisotropy present in this material.

Of more recent work directed towards an understanding of the band structure of graphite, the reflectance measurements of Taft and Philipp[8] on both natural graphite and glassy carbon, and of Carter *et al.*[9]

[1] D. G. Avery, Proc. Phys. Soc. (London) **B65**, 425 (1952).
[2] D. G. Avery, Proc. Phys. Soc. (London) **B66**, 134 (1953).
[3] P. Drude, Ann. Physik **32**, 584 (1887).
[4] R. T. Jacobsen, J. Opt. Soc. Am. **54**, 1170 (1964).
[5] R. T. Jacobsen and M. Kerker, J. Opt. Soc. Am. **57**, 751 (1967).
[6] J. T. McCartney and S. Ergun, Fuel **37**, 272 (1958).
[7] S. Ergun, Nature **213**, 135 (1967).
[8] E. A. Taft and H. R. Philipp, Phys. Rev. **138**, A197 (1965).
[9] J. G. Carter, R. H. Huebner, R. N. Hamm, and R. D. Birkhoff, Phys. Rev. **137**, A639 (1965).

on pyrolytic graphite should be mentioned. These experiments give no information on the anisotropy, but yield the optical constants for the electric vector within the planes and in addition allow a tentative explanation of the two main peaks in the reflectance spectrum at 5 and 15 eV in terms of interband transitions involving, respectively, the π and σ bands of graphite.

Calculations of the band structure of graphite using the tight-binding approach in a semiempirical way, have been performed by Bassani and Pastori Parravicini.[10] These calculations explain the main features seen in the normal incidence reflectance spectra and give a broad picture of the energy bands. A two-dimensional approximation was used, and the selection rules for optical transitions were derived within this approximation. Interactions in the z direction were not considered.

In this paper we use the analysis of the Fresnel relations to determine the optical constants both in and perpendicular to the cleavage planes of graphite. Reflectivity measurements are made as a function of the angle of incidence on the cleavage planes only. These results in conjunction with other optical and electron-energy-loss data allow a consistent picture to be presented of the band structure. The effect of the z direction (interplanar) interaction on the energy bands is also considered.

II. REFLECTIVITY AT NON-NORMAL INCIDENCE AND OPTICAL CONSTANTS

The Fresnel formulas for an anisotropic crystal have been given by Drude.[3] We report the formulas for the reflection amplitudes of a uniaxial crystal, where the c axis is perpendicular to the reflecting surface and the light is polarized with the electric vector parallel or perpendicular to the plane of incidence.

$$r_p=\frac{N_xN_z\cos\theta-(N_z^2-\sin^2\theta)^{1/2}}{N_xN_z\cos\theta+(N_z^2-\sin^2\theta)^{1/2}}, \tag{1a}$$

$$r_s=\frac{\cos\theta-(N_x^2-\sin^2\theta)^{1/2}}{\cos\theta+(N_x^2-\sin^2\theta)^{1/2}}. \tag{1b}$$

The quantities $N_x=n_x+ik_x$ and $N_z=n_z+ik_z$ indicate the complex refractive indices perpendicular and parallel to the c axis, respectively. The quantities that are measured experimentally are the reflectivities,

$$|r_p|^2=\frac{[(n_xn_z-k_xk_z)\cos\theta-\mathrm{Re}(N_z^2-\sin^2\theta)^{1/2}]^2+[(n_xk_z+n_zk_x)\cos\theta-\mathrm{Im}(N_z^2-\sin^2\theta)^{1/2}]^2}{[(n_xn_z-k_xk_z)\cos\theta+\mathrm{Re}(N_z^2-\sin^2\theta)^{1/2}]^2+[(n_xk_z+n_zk_x)\cos\theta+\mathrm{Im}(N_z^2-\sin^2\theta)^{1/2}]^2}, \tag{2a}$$

$$|r_s|^2=\frac{[\cos\theta-\mathrm{Re}(N_x^2-\sin^2\theta)^{1/2}]^2+[\mathrm{Im}(N_x^2-\sin^2\theta)^{1/2}]^2}{[\cos\theta+\mathrm{Re}(N_x^2-\sin^2\theta)^{1/2}]^2+[\mathrm{Im}(N_x^2-\sin^2\theta)^{1/2}]^2}, \tag{2b}$$

where

$$N^2-\sin^2\theta=\tfrac{1}{2}\{[(n^2-k^2-\sin^2\theta)^2+4n^2k^2]^{1/2}+(n^2-k^2-\sin^2\theta)\}^{1/2}+i\{[(n^2-k^2-\sin^2\theta)^2+4n^2k^2]^{1/2}-(n^2-k^2-\sin^2\theta)\}^{1/2}.$$

The dependence of the reflectivities on the values of the optical constants and on the angle of incidence is hidden in the rather complicated expressions (2a) and (2b), which cannot be inverted.

One can, however, use a number of approximate methods to obtain the optical constants from the experimental data at different angles. A first method can be used with a small number of measurements. It is based on successive approximations and is very useful for an immediate interpretation of experimental results since it does not require any computational facilities. The optical constants on the plane are obtained from the data with light polarized perpendicularly to the plane of incidence by an iteration procedure. One can choose an arbitrary value for n_x, and compute the corresponding k_x which gives the correct reflectivity at normal incidence according to formula (2b). Regarding the difference between the chosen values and the true values of N_x as a small perturbation, one obtains for this difference at a given value of θ

$$\frac{\Delta|r_s|^2}{|r_s|^2}=\frac{1}{|r_s|^2}\left(\frac{\partial|r_s|^2}{\partial n_x}\right)_\theta\delta n_x+\frac{1}{|r_s|^2}\left(\frac{\partial|r_s|^2}{\partial k_x}\right)_\theta\delta k_x. \tag{3}$$

The derivatives taken from (2b) give

$$\frac{1}{|r_s|^2}\frac{\partial|r_s|^2}{\partial n_x}=\frac{2}{|r_s|^2}\mathrm{Re}\left[\frac{\partial r_s}{\partial N_x}\right]$$
$$=4\cos\theta\,\mathrm{Re}[N_x(N_x^2-\sin^2\theta)^{-1/2}(N_x^2-1)^{-1}] \tag{4a}$$

and

$$\frac{1}{|r_s|^2}\frac{\partial|r_s|^2}{\partial k_x}$$
$$=-4\cos\theta\,\mathrm{Im}[N_x(N_x^2-\sin^2\theta)^{-1/2}(N_x^2-1)^{-1}]. \tag{4b}$$

Considering the angle $\theta=0$, where $\Delta|r_s|^2/|r_s|^2=0$, and a different angle, one can solve the system (3) to obtain δn_x and δk_x. This gives better values for n_x and k_x, which can be used as new starting points in the same way.

[10] F. Bassani and G. Pastori Parravicini, Nuovo Cimento 50, 95 (1967).

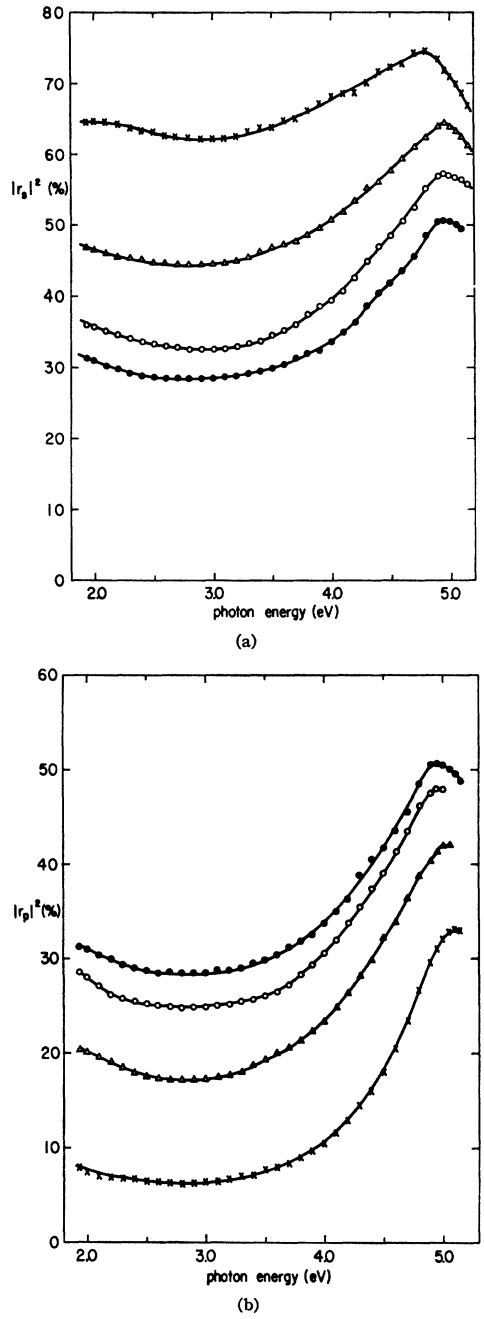

FIG. 1. Reflectivity $|r_s|^2$ (a) and $|r_p|^2$ (b) of cleaved pyrolytic graphite versus photon energy at (●) 10°, (○) 30°, (△) 50°, and (×) 70° angle of incidence.

With a few iterations one can obtain reasonable values for n_x and k_x. If the starting value for n_x was too large, then the computed curve for $|r_s|^2$ lies below the experimental one for every angle $0<\theta<\frac{1}{2}\pi$, and vice versa if the starting value for n_x was too low. Once the value N_x has been obtained, one can compute the reflectance $|r_p|^2$ for the isotropic case where $N_z=N_x$ and compare it with measured values. The deviations from isotropy are used to obtain the values for N_z in a way similar to the one previously described:

$$\frac{\Delta|r_p|^2}{|r_p|^2}=\frac{1}{|r_p|^2}\left(\frac{\partial|r_p|^2}{\partial n_z}\right)_i\delta n_z+\frac{1}{|r_p|^2}\left(\frac{\partial|r_p|^2}{\partial k_z}\right)_i\delta k_z, \quad (5)$$

where i indicates that the derivatives are computed at the initial values of the optical constants. From formula (2a) we obtain

$$\frac{1}{|r_p|^2}\frac{\partial|r_p|^2}{\partial n_z}=-\mathrm{Re}A(N_x,N_z,\theta), \quad (6a)$$

$$\frac{1}{|r_p|^2}\frac{\partial|r_p|^2}{\partial k_z}=\mathrm{Im}A(N_x,N_z,\theta), \quad (6b)$$

where

$$A=\frac{4\sin^2\theta\cos\theta N_x}{(N_z^2-\sin^2\theta)^{1/2}(N_x^2N_z^2\cos^2\theta-N_z^2+\sin^2\theta)}. \quad (6c)$$

We may notice that the experimental $|r_p|^2$ for an anisotropic material may cross the isotropic curve at most at one angle, and that such an angle can be used to obtain immediately $\delta k_z/\delta n_z$. In general one solves the system of two linear equations (5) at two different angles and obtains δn_z and δk_z, which give the new initial values for N_z. The procedure can be repeated a few times to reach consistency. In this way one obtains the optical constants with reflectivity experiments at two angles of incidence. The results, however, are rather sensitive to the values of the angles because the errors introduced by experimental uncertainties strongly depend on the angle.

To obtain more precise results for the optical constants measurements at a large number of angles are needed. One then considers the optical constants as parameters to minimize the total quadratic deviation:

$$M(n_xk_x,n_zk_z)=\sum_{i=1}^{n}[|r_{\theta i}|_{\mathrm{expt}}^2-|r_{\theta i}(n_xk_x,n_zk_z)|_{\mathrm{theor}}^2]^2. \quad (7)$$

In this way one obtains the optical constants from a numerical best fit of the experimental data. The standard library program CERN MINFUN adapted to a 7090 IBM computer has been used in the present work.

The advantage of the present analysis with respect to the previous ones[5,11] is that it can be applied to reflectivity measurements regardless of the phase relationship between r_p and r_s.

III. EXPERIMENTAL METHOD

A. Laser Measurement of Fresnel Curves

Measurements were made using a He-Ne laser (6328 Å) and also an argon ion laser (only the 5145 and

[11] A. H. Lettington, in *Optical Properties and Electronic Structure of Metals and Alloys*, edited by F. Abelès (North-Holland Publishing Co., Amsterdam, 1966), p. 147.

4579 Å lines were used for this experiment). The advantages of the lasers are not only that the light (in our case plane polarized) may be confined to a very narrow pencil, but that it is extremely easy to detect visually whether the light reflected from say a small (0.5×0.5 mm) graphite natural crystal at angles of incidence in excess of 70° is completely collected by the detector. The detector in this case was a silicon solar cell. Clearly, the use of a laser also much simplifies the problem of obtaining good absolute values of the reflectivity. The lasers moreover, enabled us to check that no significant differences existed between the optical properties of natural and pyrolytic graphite at those particular energies.

B. Spectrometer Measurement of Fresnel Curves

Fresnel curves were measured over the range from 1.9–5.15 eV using a modified Optica double-beam recording spectrometer (tungsten and D_2 lamp sources, grating, 1P28 detection). The modification included provision of an absolute reflectometer attachment having a beam focus of around 0·5×1 mm at the sample position. The beam of (monochromatic) radiation hitting the sample was limited by means of baffles to a divergence of a few degrees. The Fresnel curves shown in Fig. 1 below were measured on freshly cleaved pyrolytic graphite crystals annealed at 3600°K. The surface area of these samples (>1 cm²) and the high degree of flatness was sufficient to enable reflectivity measurements to be made accurately with incidence angles as high as 88°. The radiation from the spectrometer was polarized using a calcite air-gap Glan prism. The laser measurements provided a reliable check on the accuracy of the spectrometer curves.

C. Near-Normal Incidence Reflectivity Measurements

Samples of pyrolytic graphite having a polished face perpendicular to the cleavage planes were prepared by careful cutting and mechanical polishing techniques. No etching procedures were attempted. These samples were measured using polarized light in the Optica instrument and in a single-beam Seya-type 1-m vacuum-ultraviolet spectrometer. Polarized vacuum ultraviolet radiation was obtained by means of a single reflection from a biotite plate[12] mounted at the Brewster angle of 61°, located *before* the exit slit of the spectrometer.

All measurements reported in this present work were obtained at room temperature.

IV. EXPERIMENTAL RESULTS

Figure 2 shows the reflected intensities $|r_s|^2$, polarized perpendicularly to the plane of incidence, and $|r_p|^2$, polarized parallel to the plane of incidence, measured with 6328 Å radiation from a He-Ne laser at a number of different angles of incidence θ between 8° and 88° on freshly cleaved samples of natural single-crystal and pyrolytic graphite. We find the typical angular dependence expected from the Fresnel equations for absorbing materials with a pseudo-Brewster angle of about 75°. The curves obtained by the best-fit analysis of Sec. II are also shown in Fig. 2 and will be discussed in Sec. V. The most important fact emerging from the figure is the agreement between the reflectivity of natural single-crystal graphite and the pyrolytic graphite which we had available. The agreement is within experimental accuracy for $\theta \leqslant 80°$. (Above 80° the values obtained on natural graphite tend to be smaller because at nearly grazing incidence, the light beam is not confined within a sufficiently flat surface area of the small single crystals). The identical results obtained on the two kinds of material prove, clearly, that the optical constants of good pyrolytic graphite, for all practical purposes, are identical to those of natural single crystals. For the special case of near-normal incidence, this observation has already been made by Taft and Philipp in the energy range from 0.03–26 eV.[8] This fact enabled us to carry out the determination of the tensor components of the wavelength-dependent complex refractive index of graphite mainly on pyrolytic material.

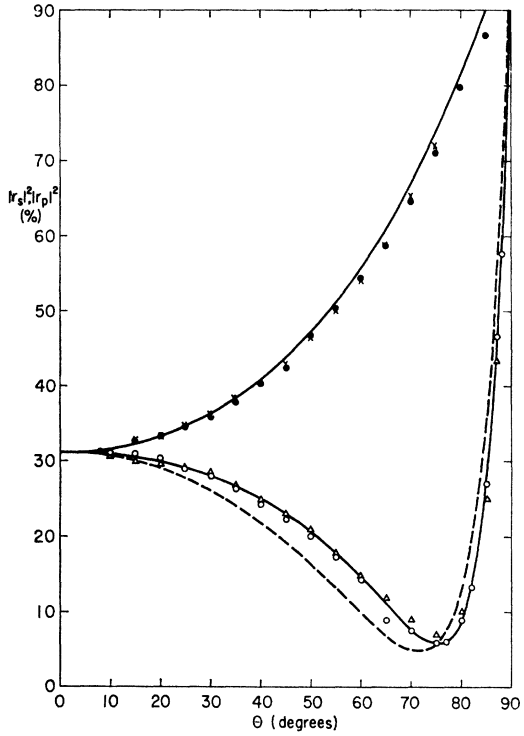

FIG. 2. Reflectivity of graphite at $\lambda = 6328$ Å ($h\nu = 1.96$ eV) versus angle of incidence. (×) reflected intensity $|r_s|^2$, polarized perpendicularly to the plane of incidence, natural graphite; (△) reflected intensity $|r_p|^2$, polarized parallel to the plane of incidence, natural graphite; (●) $|r_s|^2$, pyrolytic graphite; (○) $|r_p|^2$ pyrolytic graphite. The solid line is the theoretical curve with $n_x = 2.73$, $k_x = 1.4$, $n_z = 1.53$, $k_z = 0$. The broken line is the result one would expect for an isotropic material with $n_x = n_z = 2.73$, $k_x = k_z = 1.4$.

[12] M. B. Robin, N. A. Kuebler, and Pao Yoh-Han, Rev. Sci. Instr. 37, 922 (1966).

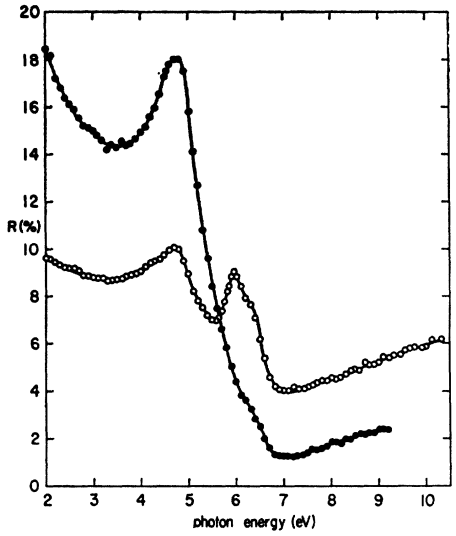

FIG. 3. Reflectivity of polished pyrolytic graphite for (●) $E\perp c$ and (○) $E\|c$ under near-normal incidence.

Similar results to those shown in Fig. 2 have also been obtained at $\lambda=5145$ Å and $\lambda=4579$ Å by use of an argon-ion laser.

We have also measured the reflected intensities $|r_s|^2$ and $|r_p|^2$ in the continuous energy range from 1.93 to 5.15 eV with incoherent light at angles from 10° to 80° in steps of 10° as well as at 75°, 85°, and 87° on freshly cleaved pyrolytic samples. For an illustration of the results, Figs. 1(a) and 1(b) show the curves taken at 10°, 30°, 50°, and 70° for $|r_s|^2$ and $|r_p|^2$, respectively. For small angles of incidence, the data are in agreement with the results obtained by Taft and Philipp[8] under near-normal incidence. With increasing angle of incidence the $|r_s|^2$ curves are shifted upwards, as we have seen in detail for $h\nu=1.96$ eV (equivalent to $\lambda=6328$ Å) in Fig. 2. It should be noted that at the same time the curves become flatter and the 5-eV maximum is shifted to smaller energies. The $|r_p|^2$ curves are shifted downwards with increasing angle of incidence θ, as long as θ is smaller than the pseudo-Brewster angle. As θ increases, the slope towards the maximum around 5 eV also increases and the position of the maximum is shifted to higher energies. Similar results have been obtained on natural single crystals but there the accuracy is insufficient for a quantitative evaluation, particularly for large angles, because of the extremely small size of suitable flat regions of the samples.

Measurements with various angles of incidence have not been performed in the vacuum uv range. In order to get an insight into the optical properties for $E\|c$ in this region we took a different approach, namely, the measurement of the reflectivity of pyrolytic graphite under near-normal incidence on a polished surface parallel to the c axis. Figure 3 shows the results for $E\perp c$ and $E\|c$ between 2 and 9 eV. Because of the inferior surface quality, the $E\perp c$ values do not reach those obtained on cleaved surfaces [see the two curves for $\theta=10°$ in Fig. 1(a), and 1(b)], but the shape of the curve and the position of the maximum are approximately the same. This kind of influence of the surface properties on the reflected intensities is often encountered in the intrinsic absorption region where the penetration depth is of the order of 100 to 1000 Å. Reflectivity spectra obtained under nonoptimum surface conditions are not suited for a determination of the optical constants by means of the Kramers-Kronig dispersion relations. It is nevertheless well justified to *compare* data taken under identical surface conditions provided the line shapes are not distorted; that this is reasonable in our case is shown by the $E\perp c$ curve in Fig. 3. We note that the $E\|c$ curve lies much lower up to energies of 5 eV and that the maximum at 4.8 eV rises only slightly above the background level at lower energies. From comparison with the $E\perp c$ curve we conclude that there is considerably less oscillator strength in the interband transitions below 5 eV for $E\|c$. This difference is even larger for the interband transitions which dominate at energies below 2 eV. The high-energy tail of these transitions out to about 3 eV in the $E\perp c$ spectrum is not found in the $E\|c$ curve. The situation is reversed for interband transitions at energies above 5.8 eV, where the $E\perp c$ curve continues to fall off steeply to very low values between 7 and 8 eV and then rises gently in good agreement with the results of Taft and Philipp. The $E\|c$ curve, on the other hand, shows a well-pronounced maximum at 6.0 eV and stays at a higher level than the $E\perp c$ curve up to 9 eV. This gives evidence for additional interband transitions at and above 6 eV, which are forbidden for $E\perp c$ and allowed for $E\|c$.

In order to check with higher accuracy the $E\perp c$ reflectivity in the region where the new $E\|c$ maximum occurs, we finally remeasured the reflectivity of cleaved natural graphite under near-normal incidence from 0.3–

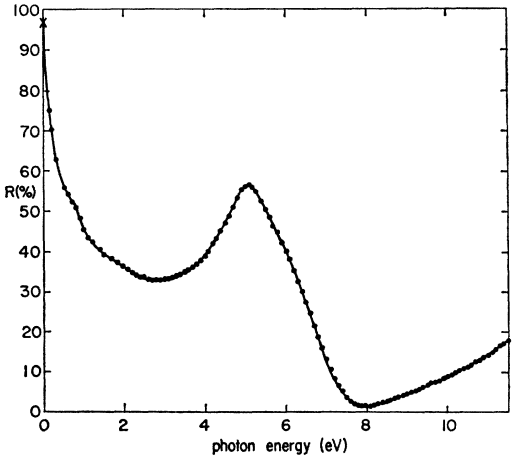

FIG. 4. Reflectivity of cleaved natural single-crystal graphite under near-normal incidence. (●) present results, (×) from Boyle and Nozières [W. S. Boyle and P. Nozières, Phys. Rev. 111, 782 (1958)].

11.5 eV. Figure 4 shows the result of these measurements. There is noticeably little scatter in the data which are in excellent agreement with the curve of Taft and Philipp with one exception. In addition to all the features that they have found, we note a marked change in slope around 6.2 eV resulting in a pronounced asymmetry in the line shape of the reflectivity maximum at 5.1 eV. We recall that this maximum is due to π-π interband transitions at a saddle point in the $(E_c - E_v)$ versus **k** function in the two-dimensional band model of Bassani and Pastori.[10]

V. ANALYSIS OF THE DATA AND DISCUSSION

We have analyzed the results of Sec. IV using the methods described in Sec. II. As an example we compare in Fig. 2 the experimental results at 1.96 eV with the curves obtained from Eq. (2) of Sec. II by the best-fit analysis of formula (7). The values of the optical constants that minimize the square mean deviation of all available data are $n_x = 2.73, k_x = 1.40, n_z = 1.53, k_z = 0$. For comparison we also report in Fig. 2 the reflectivity $|r_p|^2$ which would obtain in the isotropic case with $n_x = n_z = 2.73$ and $k_x = k_z = 1.40$. We can observe that the isotropic curve crosses the experimental curve at an angle $\theta \simeq 75°$ and is lower than the experimental curve at smaller angles. One can also note that the effect of anisotropy is already evident at small angles and that the deviations from isotropy are such that the approximate method described in Sec. II could be used with reasonable accuracy.

A similar analysis has been performed on the data of Fig. 1 at different frequencies. The optical constants on the plane and along the c axis have been obtained between 2 and 5 eV. We give in Fig. 5 the optical constants on the plane, and for comparison the values obtained by Taft and Philipp[8] from a Kramers-Kronig analysis of

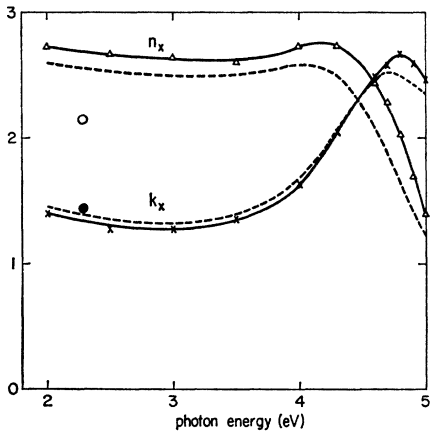

FIG. 5. Values of the optical constants n_x and k_x of graphite computed from a best-fit analysis of the results of Fig. 1. For comparison the results obtained by Taft and Phillip (Ref. 8) with a dispersion analysis of reflectivity at near-normal incidence are also indicated (broken line). The open and full circles at 2.27 eV indicate the result of Ergun (Ref. 7).

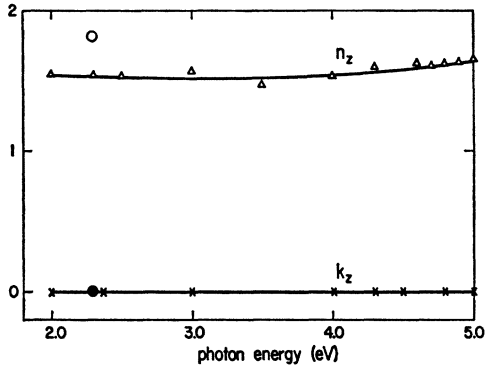

FIG. 6. Values of the optical constants n_z and k_z of graphite computed from a best-fit analysis of the data of Fig. 1. The open and full circles indicate the result of Ergun (Ref. 7).

normal incidence reflectivity. Substantial agreement is found, and this can be taken as a test of the accuracy of both approaches. In Fig. 5 the results of Ergun obtained at 2.27 eV have also been included; the n_x value shows a rather marked difference from the other two sets of data. In Fig. 6 we present the results for the optical constants along the c axis. Note that graphite is completely transparent for light polarized along the c axis up to 5 eV. The constant value of n_z is about 1.54, again somewhat different from the value 1.81 obtained by Ergun with a different procedure. The slight increase of n_z starting at about 5 eV indicates the approach of an absorption edge at higher energies.

The results of Fig. 6 can be interpreted on the basis of the band structure in the two-dimensional approximation as was the case for the optical constants on the plane.[10] For the sake of illustration we reproduce in Fig. 7 the Brillouin zone (BZ) of graphite, and in Fig. 8 illustrate the semiempirical band structure recently computed[10] in the two-dimensional approximation. In this case transitions between π bands are forbidden when light is polarized with the electric vector parallel to the c axis. Consequently the optical constants n_z and k_z are due only to transitions between σ and π bands. The results of Fig. 6 indicate that the separation between the lowest π conduction band and the highest σ valence band is larger than 5 eV. This is in agreement with the results of Ref. 10 shown in Fig. 8, indicating that the lowest energy transitions contributing to k_z should take place only above 6 eV. We feel that the 6.0-eV peak in the $E \| c$ curve in Fig. 3 gives evidence of transitions of that energy, which are forbidden for $E \perp c$. Though in such cases there is some mixture of the two optical constants, the peak at 6.0 eV with $E \| c$, which is not present for $E \perp c$, can only be due to a structure in N_z. This could also explain the slight bump at 6.8 eV in the unpolarized reflectivity at 70° obtained by Carter *et al.*[9] Further evidence of an increase in k_z above 6 eV is provided by a recent analysis of electron-energy-loss data,[13] which gives information on the

[13] F. Bassani and E. Tosatti, Phys. Letters 27, 446 (1968).

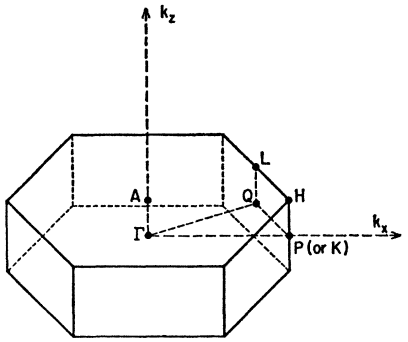

FIG. 7. Three-dimensional BZ of graphite.

optical constants at energies above 6 eV. Though the available data are not sufficient to compute the values of the optical constants N_z in the region around 6 eV, we can safely assume here a weak peak in k_z. This weak structure can be attributed to transitions between the highest σ valence band and the lowest π conduction band, the lower oscillator strength of this maximum as compared to the other saddle-point transition peaks being due to the selection rules which make the transition forbidden at the critical points P and Q.

A much stronger peak in ϵ_{2z} at 11 eV has resulted from the analysis of the energy-loss spectra;[13] its occurrence is also indicated by the increase of the $E\|c$ reflectivity towards 10 eV in Fig. 3. Since the peak is comparable in oscillator strength to the Q_{2g}^--Q_{2u}^- singularity it is most probably also caused by saddle-point transitions which in the two-dimensional model occur only at Q. Out of the possible π-σ (or σ-π) transitions at Q, the Q_{2u}^+-Q_{2u}^- and the Q_{2g}^--Q_{2g}^+ transitions are forbidden by selection rules as indicated in Fig. 8. The lowest-energy saddle-point transitions allowed for $E\|c$ which could give rise to the 11-eV peak are Q_{1g}^+-Q_{2u}^-. This energy separation has originally been calculated to have a value of about 13 eV, but a rigid shift of $\sim$2 eV of the σ bands relative to the π bands is not unlikely. A further possibility is an allowed transition at the saddle point Q between the highest π valence band and a σ conduction band (Q_{2g}^--Q_{1u}^+). The position of the conduction-band state Q_{1u}^+ has not been marked accurately in Fig. 8 but from the tight-binding calculation it can be shown to occur slightly above the Q_{1g}^+ state. The energy separation for such a transition is larger than Q_{1g}^+-Q_{2u}^- on the basis of the two-dimensional calculation,[10] but the tight-binding scheme is not very reliable for conduction states, and this possibility cannot be completely ruled out. A different interpretation has been advanced by Phillips,[14] who suggests that the selection rules can be sufficiently relaxed in the vicinity of the points Q and P to allow a sharp peak due to transitions between the highest σ band and the lowest π band. These transitions could be degenerate with the analogous π-σ transitions between bonding and antibonding states.[14] We do not think this is a likely alternative for the 11-eV peak because of its high oscillator strength, though this is probably the situation for the low-intensity structure in k_z above 6 eV.

We now turn to the shoulder at 6.2 eV in Fig. 4. According to the selection rules given in Ref. 10, the zone-center transitions Γ_{3g}^+-Γ_{3u}^+ are allowed for $E\perp c$: These transitions (of type M_0) should occur around 6 eV. In fact we can present two possible pieces of evidence for the presence of such transitions. Firstly, the observed asymmetry of the 5-eV peak revealed in Fig. 4 is indication that some weak structure is present around 6.2 eV. The low oscillator strength of these zone-center transitions is understandable in terms of comparison with the strength observed for all M_0 transitions in the diamond and zincblende materials. Secondly, the thermoreflectance results of Balzarotti and Grandolfo[15] indicate an allowed transition for $E\perp c$ at 5.96 eV. It may not in fact be surprising that a strong thermoreflectance signal is observed where no sharp structure is observed in the direct reflectance. The strength of the thermoreflectance signals will depend on the values of the various deformation potentials for the bands involved, whereas the direct reflectance signal will depend on the joint density of states.

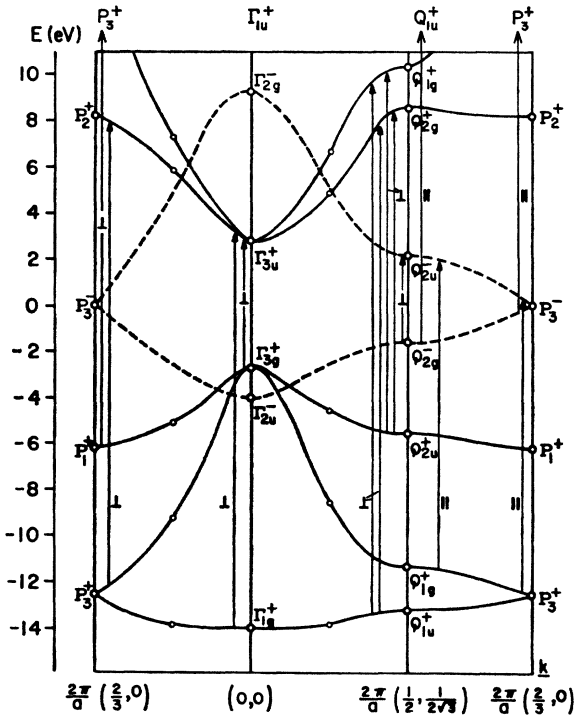

FIG. 8. Band structure of two-dimensional graphite after Bassani and Pastori (Ref. 10). σ and π bands are indicated by continuous and broken lines, respectively. The allowed transitions at critical points are indicated for both polarizations.

[14] J. C. Phillips (private communication).

[15] A. Balzarotti and M. Grandolfo, Phys. Rev. Letters 20, 9 (1968).

TABLE I. Values of the two-center integrals considered in the calculation of three-dimensional π bands in graphite (energies in rydbergs). The symbols $S(\ )$ indicate overlap integrals of p_z functions with quantization axis perpendicular (σ) or parallel (π) to the vector joining the two lattice sites. The potential in the integrals $V(\ )$ is centered on one of the lattice sites. The subscript 1 indicates nearest sites on the same plane, and Roman subscripts I and II indicate nearest and next-nearest sites on different planes. The subscripts α and β in the crystal-field integrals indicate that the two lattice sites in the unit cell are not equivalent in the three-dimensional case. The difference reported in the table corresponds to the parameter Δ used by many authors.[a]

Overlap integrals	Potential integrals
$S_1(pp\pi) = 0.170$	$V_1(pp\pi) = -0.160$
$S_1(pp\sigma) = -0.029$	$V_1(pp\sigma) = 0.015$
$S_{II}(pp\sigma) = 0.017$	$V_{II}(pp\sigma) = 0.007$
Difference of crystal-field integrals $(p_z^2 \sum' V_a)_\alpha - (p_z^2 \sum' V_a)_\beta = 0.0002$	

[a] Reference 17.

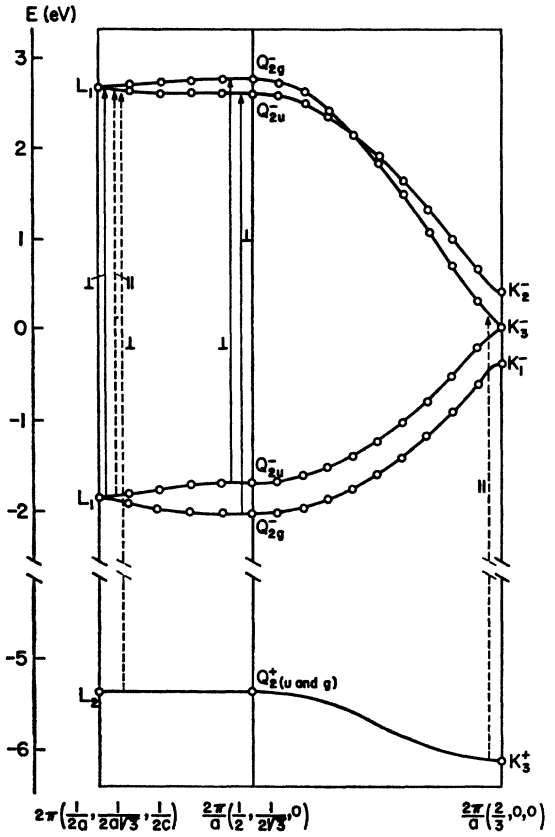

FIG. 9. Band structure of three-dimensional graphite in the directions QL and QK of the BZ computed with the parameters of Table I. The positions of the σ bands are taken from Bassani and Pastori (Ref. 10). The effect of the interaction between adjacent planes has been estimated for the π bands by including nearest and next-nearest integrals. The continuous arrows indicate transitions at the symmetry points that are allowed in the three-dimensional approximation and also in the two-dimensional approximation. The broken arrows indicate transitions that are allowed only in the three-dimensional approximation (much weaker). The polarization of the light relative to the c axis is indicated by the direction of the electric field.

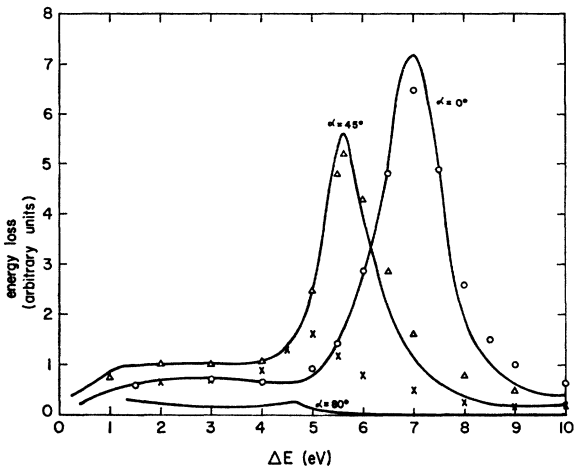

FIG. 10. Electron energy loss of 60-keV electrons computed from the optical constants of Figs. 5 and 6 with three different angles of incidence and a detection angle $\theta = 10^{-3}$ rad shown as continuous lines. Experimental points taken from the data of Zeppenfeld (Ref. 18) are indicated for comparison, (○) $\alpha = 0°$, (△) $\alpha = 45°$, (×) $\alpha = 80°$.

We have not considered so far the effect of the interaction between the planes. The experimental evidence indicates that this is a very small effect since the peak in ϵ_{2x} at 4.6 eV does not show the doublet structure which would appear because of the splitting of the π states by the interaction between planes. However it has been shown that the interaction between planes produces splittings of nearly 1 eV at the point P of the BZ,[16,17] and similar splittings should occur and be observable at point Q. To understand why splittings are not observed we have undertaken a three-dimensional calculation of the π bands of graphite at all points of the BZ. The σ bands are certainly affected to a much smaller extent, and have not been considered. We use the tight-binding scheme, taking into account overlap between p_z functions on different planes as computed from Slater atomic functions, and potential integrals proportional to the values computed from the above wave functions and Hartree atomic potentials. The multiplying factor was chosen to reproduce the splittings of the states at the Fermi surface.[16] The numerical values of the two-center integrals used in the calculation are given in Table I. Note that the potential integrals in this case are larger than the values computed from atomic functions by a factor of 4. The results obtained at the symmetry points and symmetry lines of interest are given in Fig. 9, where the relevant selection rules at critical points are also indicated for both polarizations. The absence of the doublet at the saddle-point transition at 4.6 eV is due to the degeneracy at the point L, and to the fact that the order of even and odd states is opposite in the valence and the conduction bands at the point Q.

[16] J. W. McClure, Phys. Rev. **108**, 612 (1957).
[17] G. Dresselhaus and M. S. Dresselhaus, Phys. Rev. **140**, A401 (1965).

This explains why the two-dimensional approximation is more accurate than expected. We also wish to remark that transitions between π bands are not strictly forbidden for light parallel to the c axis in the three-dimensional approximation (see e.g., L_1-L_1). However the result of Fig. 6 indicates that their oscillator strength is negligible because k_z is zero below 6 eV, and this gives a further justification of our attempt to explain all the optical properties in the fundamental absorption region within the two-dimensional model.

VI. OPTICAL CONSTANTS AND ELECTRON ENERGY LOSS

The results of Sec. V can be used to interpret energy-loss experiments recently performed on graphite by Zeppenfeld.[18] The electron beam impinges on the foil at an angle α with respect to the c axis and is detected at an angle θ from the incident direction. The transition rate for the transfer of momentum $\hbar\mathbf{q}$ and energy $\hbar\omega$ is given by[13]

$$W_{\alpha\theta}(\mathbf{q},\omega) = -(8\pi e^2/\hbar)\,\mathrm{Im}[(\epsilon_x q_x^2+\epsilon_z q_z^2)^{-1}]. \quad (8)$$

Here $\epsilon=(n+ik)^2$, $q_x=q_{\parallel}\sin\alpha-q_{\perp}\cos\alpha$, $q_z=q_{\parallel}\cos\alpha+q_{\perp}\sin\alpha$, and $q_{\parallel}=\omega/v$, $q_{\perp}=m_e v\theta/\hbar$ indicate the momentum transfer parallel and perpendicular to the electron beam, respectively (v is the velocity of the electrons). In Fig. 10 we give the energy loss at three different angles of incidence, computed with formula (8) and the values of the optical constants of Taft and Philipp[8] and of Fig. 6. We did not attempt to include the variation of ϵ_z between 5 and 10 eV, but simply used $\epsilon_z=2.5$, because this approximation seems sufficient to give the main experimental features. For comparison some experimental points are also indicated in Fig. 10. The agreement between theory and experiment is quantitatively accurate for $\alpha=0°$ and $\alpha=45°$, but is only qualitative for $\alpha=80°$, probably because at this angle of incidence there is some uncertainty about the magnitude of q_x.

The main result that emerges from the present analysis of the energy-loss data is that there is no plasmon in the direction of the c axis, corresponding to the plasmon at 7 eV for momentum transfer in the plane. The shift and decrease of this peak as the angle of incidence increases, is not due to a plasma anisotropy but to the interband transitions responsible for the peak in ϵ_{2x} at 4.6 eV. In fact, increasing the angle of incidence amounts to decreasing the momentum transfer in the plane and increases the role of ϵ_z with respect to ϵ_x in formula (8). Even at 80° there is a small peak corresponding to the optical transitions on the plane, but any other structure has been completely masked by ϵ_z.

VII. CONCLUSIONS

In the present work we have developed a method of analysis of the Fresnel relations for a uniaxial material, to give the optical constants both perpendicular and parallel to the crystal planes. This method has been employed in the case of graphite. No significant differences are found between the optical properties and hence band structure of natural and pyrolytic graphite. The Fresnel analysis indicates that, as might be expected, strong anisotropy does exist, and in particular $\epsilon_{2z}=k_z=0$ and $\epsilon_{1z}=\text{const}=2.35$ for $h\nu\lesssim 5$ eV. The frequency-dependent values for ϵ_{1x} and ϵ_{2x} are in close agreement with results reported previously for the special case of near-normal incidence with the application of Kramers-Kronig dispersion relations. The tensorial dielectric constant obtained by our method has been used by Phillips[19] to estimate the bonding charge in the planar (sp^2) bonding in graphite as compared to the tetrahedral (sp^3) bonding in diamond.

In conjunction with other optical data and electron-energy-loss data, the results of the Fresnel analysis yield a consistent picture of the fundamental band structure. The band structure of graphite can be adequately interpreted in terms of a two-dimensional model. In particular, the following scheme for interband transitions is proposed:

0 eV	P_3^- state (the "zero-energy gap" of graphite);
4.6 eV	Q_{2g}^--Q_{2u}^- transitions, allowed for $E\perp c$;
$\simeq$6 eV	Γ_{3g}^+-Γ_{3u}^+ transitions, allowed for $E\perp c$;
$\simeq$6 eV	Q_{2u}^-, P_1^+-Q_{2u}^-, P_3^- transitions, forbidden at Q and P, allowed along the line for $E\|c$;
$\simeq$11 eV	Q_{1g}^+-Q_{2u}^- or Q_{2g}^--Q_{1u}^+ transitions, allowed for $E\|c$;
$\simeq$14 eV	Q_{2u}^+-Q_{2g}^+ transitions, allowed for $E\perp c$.

ACKNOWLEDGMENTS

We are indebted to Dr. G. Montet, Argonne National Laboratories, for providing us with natural single crystals of graphite; and to Dr. H. E. Philipp, General Electric Research Center; and Dr. K. Zeppenfeld, University of Hamburg, for samples of pyrolytic graphite. We also gratefully acknowledge stimulating discussions with Professor J. C. Phillips and the assistance of E. Meier in sample preparation and measurements.

[18] K. Zeppenfeld, Z. Physik **211**, 391 (1968).

[19] J. C. Phillips, Phys. Rev. **168**, 912 (1968).